Journal of
Environmental
Nanotechnology

Research Article

Electrochemical Study of Inhibition of Corrosion of Copper by Ofloxacin in Acid Media

P. Thanapackiam*, E. P. Subramaniam, K. V. Hemalatha, B. Gayathri
Department of Chemistry, Coimbatore Institute of Technology, Coimbatore, TN, India
Received: 08.09.2018 Accepted: 22.11.2018 Published: 30-03-2019
*pthanapackiam@rediffmail.com

ABSTRACT

The inhibition efficiency of ofloxacin, a fluoroquinolone, on the corrosion of copper in acids has been studied employing polarisation, EIS and weight loss measurements. Ofloxacin had a high inhibition effectiveness, and the inhibitory activity was mixed in nature but mainly cathodic in character. The method of inhibitor adsorption onto the metal surface was identified by determining the potential of zero charges. The activation energy (E_a) and thermodynamic parameters such as the adsorption equilibrium constant (K_{ads}) and the free energy of adsorption (ΔG_{ads}) were estimated using the temperature dependence of corrosion rates. The fact that the free energy of adsorption is near to -40 $kJmol^{-1}$ showed that adsorption occurred *via* electrostatic coulombic attraction and chemisorption and that the Langmuir adsorption isotherm was followed. Among the potassium halides, only KI improved the inhibition efficiency of ofloxacin by synergism. The structural features obtained by quantum chemical calculations were also supportive of the experimental results.

Keywords: Adsorption; Corrosion; Copper; Ofloxacin; Potentio-dynamic polarisation; Thermodynamic properties.

1. INTRODUCTION

Copper metal plays an important role in chemical and electronic fields due to its high electrical and thermal conductivity. Copper is one of the noble metals which require strong oxidants for its corrosion. The major methods used in the production of electrical devices are electrolytic plating and chemical dissolution. Since nitric acid is the most often used corrosive solution, it has sparked a lot of interest in copper corrosion research. Chemical inhibitors are one of the most practical strategies for preventing corrosion in acidic environments.

In this work, inhibition efficiency of ofloxacin for corrosion of copper in 1.0 M HNO_3 and 0.5 M H_2SO_4 acid solutions were studied. Various techniques like electrochemical impedance spectroscopy and potentio-dynamic polarization were employed and adsorption studies were carried out. The different thermodynamic parameters were calculated and discussed.

2. EXPERIMENTS

2.1 Materials and Reagents

Copper specimens of dimensions 2.5 cm x 1 cm x 0.1 cm were used for weight-loss measurements. It has a composition of 99.5 wt. % Cu, 0.003 wt. % Ni, 0.116 wt. % Si, 0.019 wt. % Al and 0.002 wt. % Mn. These specimens were polished with various grades of emery sheets, then washed in acetone and dried. For electrochemical investigations, a Teflon-coated cylindrical copper electrode of the prior composition was utilized. All the chemicals used were of analytical reagent grade (Sigma Aldrich) and E Merck (India). Inhibitor stock solutions of concentration 2.5 M were prepared with respective acids.

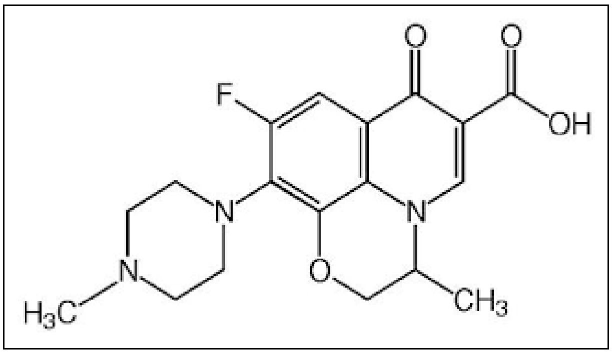

Fig. 1: Structure of ofloxacin.

2.2 Weight Loss Measurements

In the blank and with the inhibitor, the copper specimens were submerged in 100 ml of acid medium at room temperature for 2 h. The inhibitory effectiveness was calculated using the method based on the average weight loss:

$$IE = \left(\frac{W-W'}{W}\right) \times 100 \qquad (1)$$

where, w and w' represent the corrosion rates in the uninhibited and inhibited solutions, respectively.

2.3 Electrochemical Impedance Measurements

Electrochemical experiments were conducted using a three-electrode system. The auxiliary electrode was a Pt foil, the reference electrode was a saturated calomel electrode (SCE) and the working electrode was a Teflon-coated copper rod. After immersing the specimen in the corrosive medium, the specimen was given a 45-minute stabilization period. A potentiostat (GAMRY REFERENCE 600) was used to measure electrochemical impedance, and the data were analyzed using Gamry Echem Analyst software. The expression used to compute inhibition efficiencies (IE %). (Doner *et al.* 2011) is:

$$IE\ \% = \frac{R'_{ct} - R_{ct}}{R'_{ct}} X100 \qquad (2)$$

where, R_{ct} and R'_{ct} are the charge transfer resistance values in the uninhibited and inhibited solutions respectively.

2.4 Polarization Measurements

The same cell was used to record potentio-dynamic polarisation curves at a potential sweep rate of 1.6 mVs^{-1}. The potentials were scanned largely from negative to positive potentials through OCP, with E_{corr} and i_{corr} values generated from the polarisation curves. Using the connection, the inhibition efficiencies were computed (Sahin *et al.* 2002).

$$IE\% = \frac{i_{corr} - i'_{corr}}{i_{corr}} \text{X } 100 \qquad (3)$$

where, i_{corr} and i'_{corr} are the corrosion current densities in the blank and in the presence of inhibitor, respectively.

2.5 Study of Synergistic Effect of Halide Ions

The synergistic effect was studied using KCl, KBr and KI. Aramki and Hackermann equation (Aramaki and Hackerman, 1969) was used to calculate S_θ as given below:

$$S_\theta = \frac{1-\theta_{1+2}}{1-\theta'_{1+2}} \qquad (4)$$

where, $\theta_{1+2} = (\theta_1 + \theta_2) - (\theta_1\theta_2)$; θ_1 = surface coverage by anion; θ_2 = surface coverage by cation; θ'_{1+2} = measured surface coverage by both cation and anion.

2.6 Determination of Activation Energy

The activation energy for the adsorption of the inhibitor onto the copper surface was estimated using the Arrhenius equation in the presence and absence of the inhibitor in the temperature range of 308 to 328 K in both the acid solutions:

$$i_{corr} = A\ e^{-Ea/RT} \qquad (5)$$

where, i_{corr} is the corrosion current density, A is the Arrhenius pre-exponential constant, E_a is the energy of activation, R is the universal gas constant and T is the absolute temperature.

2.7 Measurement of Potential of Zero Charge (PZC)

Electrochemical impedance values were recorded at 20 kHz AC frequency after varying the applied DC potentials. PZC was obtained from the lowest point of the plot of differential capacitances vs. DC potential.

2.8 Surface Morphology Studies

A digital Scanning Electron Microscope was used to examine the surface morphologies of the corroded samples in the blank and in the presence of the inhibitor. At a magnification of 200X, all micrographs were obtained.

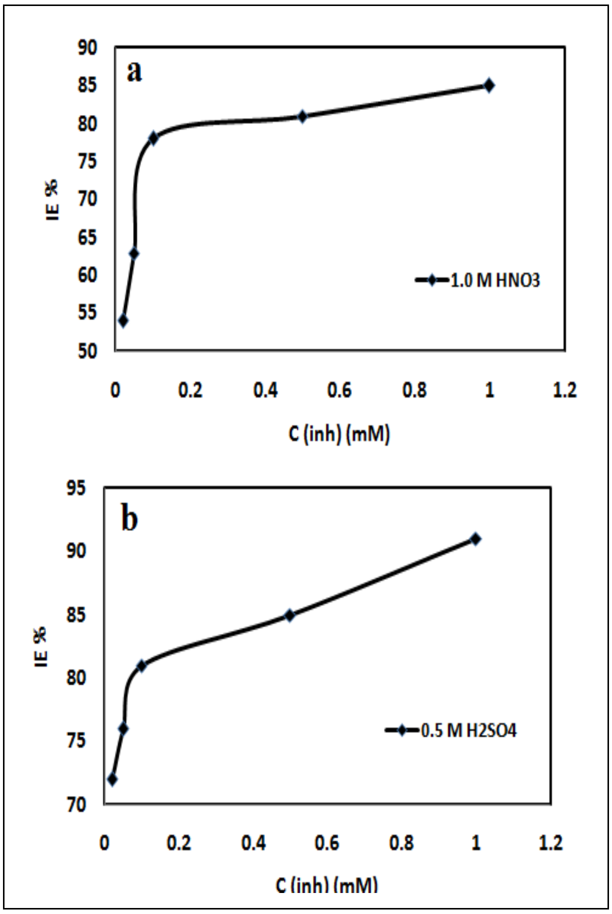

Fig. 1: Plots of inhibitor efficiency (%) with concentration of ofloxacin in: (a) 1.0 M HNO_3 and (b) 0.5 M H_2SO_4 media.

2.9 Quantum Chemical Calculations

The structures were optimized first, and then simulations were run to determine the electronic characteristics. The quantum chemical calculations were done using the Semi-empirical method - Parameterized Model 3 (PM3) (Gao, 1996). Density functional theory (DFT) (Geerlings *et al.* 2003) has been found to be successful in providing all the theoretical parameters.

3. RESULTS AND DISCUSSION

3.1 Weight Loss Neasurement

Table 1 gives the inhibition efficiencies at different concentrations of the inhibitor. Because a considerable portion of the surface was already covered by the inhibitor *via* adsorption, the inhibition effectiveness was shown to rise with the concentration of the inhibitor, especially sharply at first dosages but tending to reach a constant value, as shown in Fig. 1 (a and b). The curve flattened out when the dosage was increased, indicating Type I adsorption and roughly 90% inhibition was reached at 1.0 mm.

3.2 Electrochemical Impedance Study

The impedance spectra measured in 1.0 M nitric acid and 0.5 M sulphuric acid solutions at varied doses of the inhibitor are shown in Fig. 2 (a and b). Depressed semi-circles were formed as a result of non-ideal capacitance action at electrochemical solid/liquid interfaces (Hosseini *et al.* 2003). Roughness, chemical inhomogeneities, degree of polycrystallinity and anion adsorption were the major causes of capacitance dispersion at solid surfaces (Rahman *et al.* 1997). The impedance spectrum has shown a high-frequency capacitive loop and the Warburg impedance at low frequencies, which may be examined using the analogous circuit shown in Fig. 3 (Khaled, 2010; Ma *et al.* 2002).

Table 1 Inhibitor efficiency from weight loss measurement for copper in 1.0 M HNO_3 and 0.5 M H_2SO_4 solutions at different concentration of the inhibitor.

Medium	Inhibitor concentration (mM)	Corrosion rate (mmpy)	Inhibitor efficiency (IE%)
1.0 M HNO_3	Blank	47.2162	-
	0.02	21.5828	54.3
	0.05	17.4167	63.1
	0.1	10.5889	77.6
	0.5	9.1423	80.6
	1.0	7.0592	85.0
0.5 M H_2SO_4	Blank	22.3929	-
	0.02	6.3649	71.6
	0.05	5.3233	76.2
	0.1	4.1661	81.4
	0.5	3.2981	85.3
	1.0	2.0830	90.7

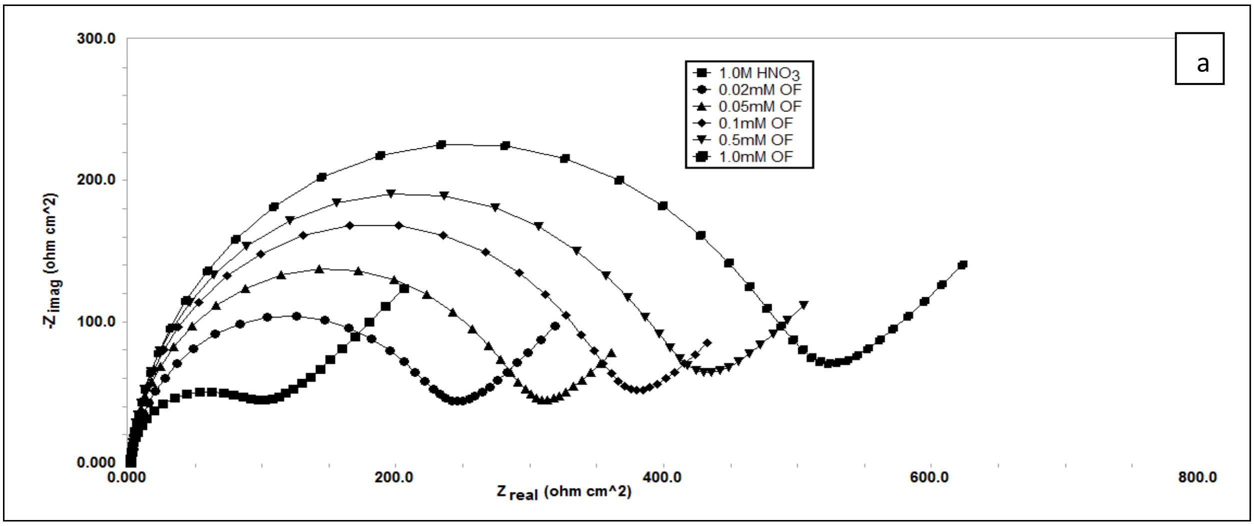

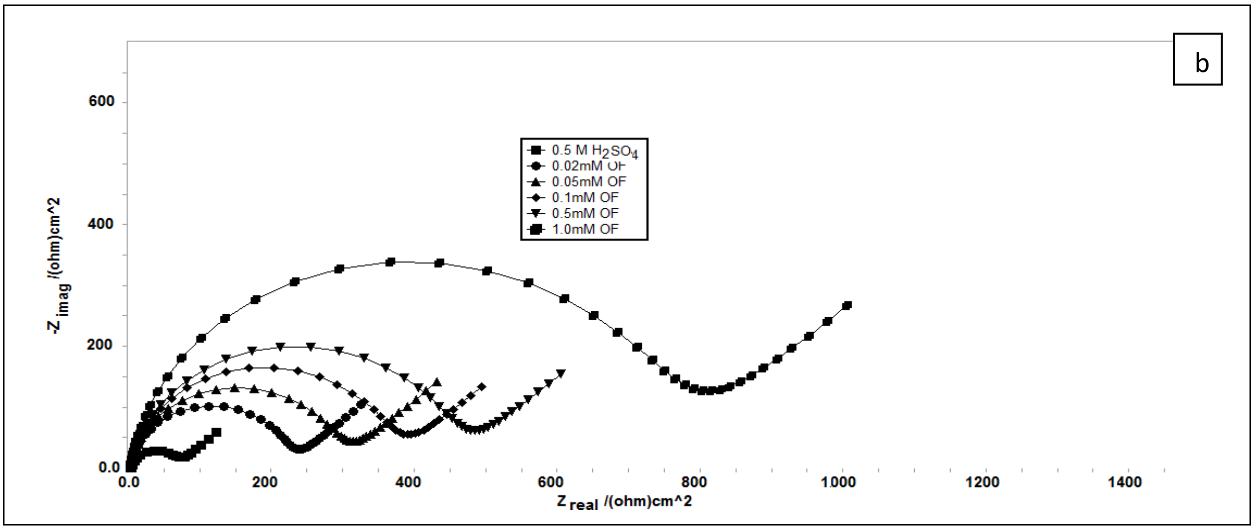

Fig. 2: The Nyquist plots for Cu electrode obtained in (a) 1.0 M HNO_3 (b) 0.5 M H_2SO_4 solutions at various concentrations of ofloxacin.

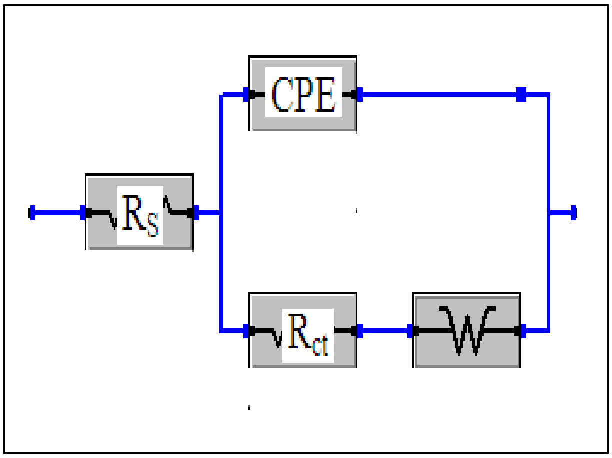

Fig. 3: Randles Equivalent Circuit for the corrosion of copper in acid media.

Angular frequency and C_{dl} are calculated using the following equation (Hsu and Mansfeld, 2001):

$$\omega_{max} = \left(\frac{1}{R_{ct}Y_0}\right)^{1/n} \quad (6)$$

$$C_{dl} = Y_0\,(\omega_{max})^{n-1} \quad (7)$$

The R_{ct} values increased with an increase in inhibitor concentrations, whereas the values of C_{dl} decreased in both the media. An increase in the R_{ct} was due to the increase in the surface coverage by the inhibitor. The decrease in C_{dl} resulted from the adsorption of the inhibitor molecule with water replacement at the metal/solution interface and decreased the rate of corrosion (Benabdellah *et al.* 2007).

Table 2. Electrochemical parameters derived from EIS measurements for the corrosion of copper in 1.0 M HNO_3 and 0.5 M H_2SO_4 solutions at different concentrations of the inhibitor.

Medium	Inhibitor Concentration (mM)	R_{ct} Ωcm^2	Y_0 (x 10^{-6}) $\Omega^{-1}cm^{-2}$	n	C_{dl} μFcm^{-2}	Inhibitor Efficiency (IE%)
1.0 M HNO_3	Blank	87.0	862.0	0.99	146	-
	0.02	223.7	366.2	0.93	102	61
	0.05	286.0	308.2	0.96	89	70
	0.10	351.0	265.2	0.96	75	75
	0.50	398.0	179.7	0.95	58	78
	1.0	487	128.4	0.94	49	82

0.5 M H_2SO_4	Blank	63.0	330.0	0.93	159	-
	0.02	221.0	93.4	0.91	118	72
	0.05	290.5	90.7	0.92	91	78
	0.10	362.0	89.0	0.92	73	83
	0.50	451.9	92.0	0.94	51	86
	1.0	749.1	70.2	0.92	24	92

3.3 Polarization Measurements

The potentio-dynamic polarisation curves in Fig. 4 (a and b) indicate the effect of the inhibitor on the anodic and cathodic Tafel slopes. The cathodic curve, on the other hand, was more influenced. The cathodic polarisation curves were almost parallel, demonstrating that hydrogen evolution was controlled by activation (Zarrouk *et al.* 2012). According to Corrosion theories (Barcia *et al.* 1993), (Barcia and Mattos, 1990), the rightward shift of the cathodic curves has revealed that the corrosion was mainly accelerated by cathodic reactions. If the difference in E_{corr} between the inhibited and uninhibited solution was higher than 85 mV, the inhibitor can be classified as either cathodic or anodic (Li *et al.* 2008; Li *et al.* 2009; Ferreira *et al.* 2004). In the current investigation, the maximum shift of E_{corr} in the presence of inhibitor in both medium was less than 85 mV, indicating that the inhibitor was of mixed type (Zarrouk *et al.* 2012).

Because there was no sharp slope in the anodic range of the polarisation curves, no passive film was formed on the copper surface. Cu^{+2} was not detected in de-aerated acid solutions, although Cu dissolved in the presence of dissolved oxygen, forming Cu^{+2} ion *via* the method described below:

Anodic reaction:

$$Cu \rightarrow Cu^{2+} + 2e^{-} \tag{8}$$

Cathodic reaction:

$$O_2 + 4H^{+} + 4e^{-} \rightarrow 2H_2O \tag{9}$$

The diffusion of soluble Cu^{+2} species from the outer Helmhotz plane to the bulk solution (Ferreira *et al.* 2004) has controlled the dissolution of copper.

Table 3 shows that when the inhibitor concentration rises, β_c and β_a change. The higher the β_c, the greater the impact on cathode reaction retardation over anodic reaction retardation (Sanghvi *et al.* 1997); implying that ofloxacin has a greater impact on the cathodic response than on the anodic response.

3.4 Mechanism of Adsorption

During the adsorption of inhibitor molecules at the metal solution interface, an organic substance (org_{sol}) from the aqueous media has displaced the water molecules connected with the metal surface (H_2O_{ads}).

$$Org_{(sol)} + xH_2O_{ads} \rightarrow Org_{ads} + xH_2O \tag{10}$$

where, 'x' indicates the number of water molecules displaced by one nano-size ofloxacin molecule. The surface coverage (θ) of the inhibitor was calculated using the relation,

$$\theta = \frac{R'_{ct} - R_{ct}}{R'_{ct}} \tag{11}$$

where, R'_{ct} and R_{ct} are the charge transfer resistance values in the inhibited and uninhibited solutions, respectively. Analysis showed that the adsorption followed Langmuir isotherm, given by the expression (Zarrouk *et al.* 2012; Joseph and Joseph, 2011),

$$C_{inh}/\theta = C_{inh} + 1/K_{ads} \tag{12}$$

and the plots are shown in Fig. 5, where C_{inh} is the concentration of the inhibitor, θ is the surface coverage, and K_{ads} is the adsorption equilibrium constant. At constant temperature, the value of K_{ads} is determined from the plot of C_{inh} vs. C_{inh}/θ. The standard free energy of adsorption is calculated using the expression:

$$K_{ads} = 1/55.5\, \exp^{-\Delta G/RT} \tag{13}$$

where, ΔG is the free energy of adsorption, T is the temperature, R is the universal gas constant, and 55.5 is the concentration of water in mol L^{-1}. The plots obtained were linear with correlation coefficients greater than 0.9. The calculated values of ΔG_{ads} at room temperature in 1.0 M nitric acid and 0.5 M sulphuric acid solutions were -39.15 $kJmol^{-1}$ and -42.84 $kJmol^{-1}$, respectively. The negative values of ΔG_{ads} show the spontaneous adsorption of ofloxacin molecules onto the metal surface. In general, $-\Delta G_{ads}$ less than and around 20 kJ mol^{-1} represents physisorption, while a value greater than 40 $kJmol^{-1}$ represents chemisorption. If $-\Delta G_{ads}$ lies between 20 $kJmol^{-1}$ and 40 $kJmol^{-1}$, it represents both physisorption and chemisorption (Joseph and Joseph, 2011; Yurt *et al.* 2005; Quraishi *et al.* 2000). Thus, in the present study, the ofloxacin molecules get adsorbed onto the metal surface by both types of adsorptions but with a higher contribution from chemisorption (Bentiss *et al.* 1999).

Table 3. Electrochemical parameters for the corrosion of copper in 1M HNO_3 and 0.5M H_2SO_4 solutions at different concentrations of the inhibitor, derived from Tafel polarization curves.

Medium	Concentration (mM)	E_{corr} (mV)	i_{corr} (µA cm^-2)	β_cx10^{-3} (V)	β_a x 10^{-3} (V)	Corrosion rate (mpy)	IE%
HNO_3	Blank	42.10	116	429.5	67.74	187.8	-
	0.02	-3.28	34.4	259.5	60.70	55.67	70
	0.05	-0.69	30.0	308.9	55.10	48.51	74
	0.1	-1.08	25.2	282.7	60.00	40.75	78
	0.5	-3.03	21.5	244.8	51.00	34.92	81
	1.0	-14.3	18.2	226.4	59.92	29.48	84
H_2SO_4	Blank	4.52	172.0	714.3	84.67	81.35	-
	0.02	-11.90	25.2	666.3	43.30	40.75	85
	0.05	-18.30	21.5	527.1	45.10	34.92	87
	0.1	-18.90	15.1	430.7	50.50	24.47	91
	0.5	-18.90	9.82	407.8	45.80	15.89	94
	1.0	-22.44	6.91	358.8	45.21	11.78	96

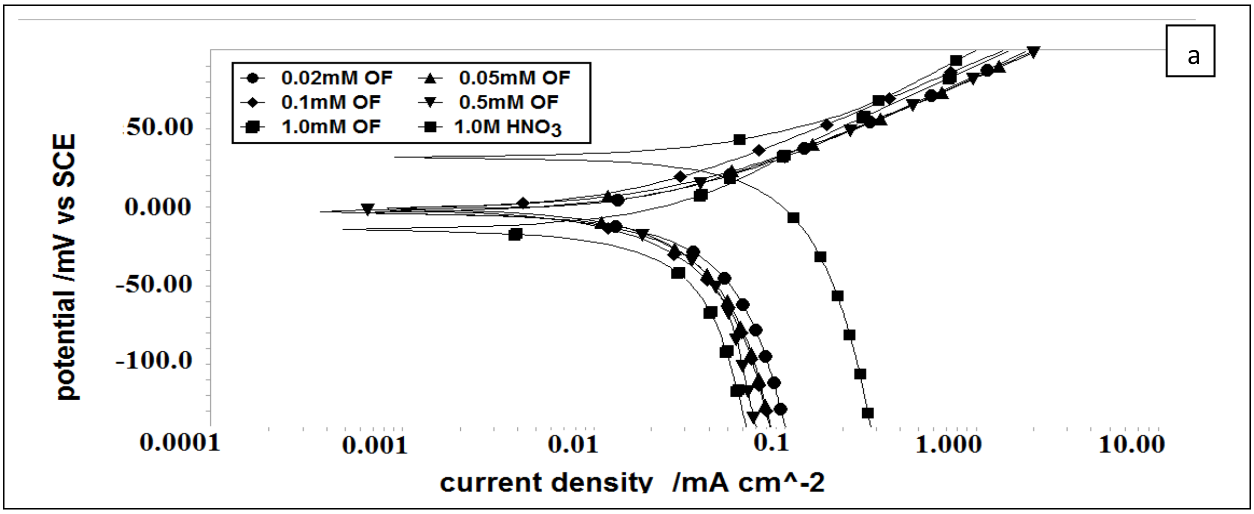

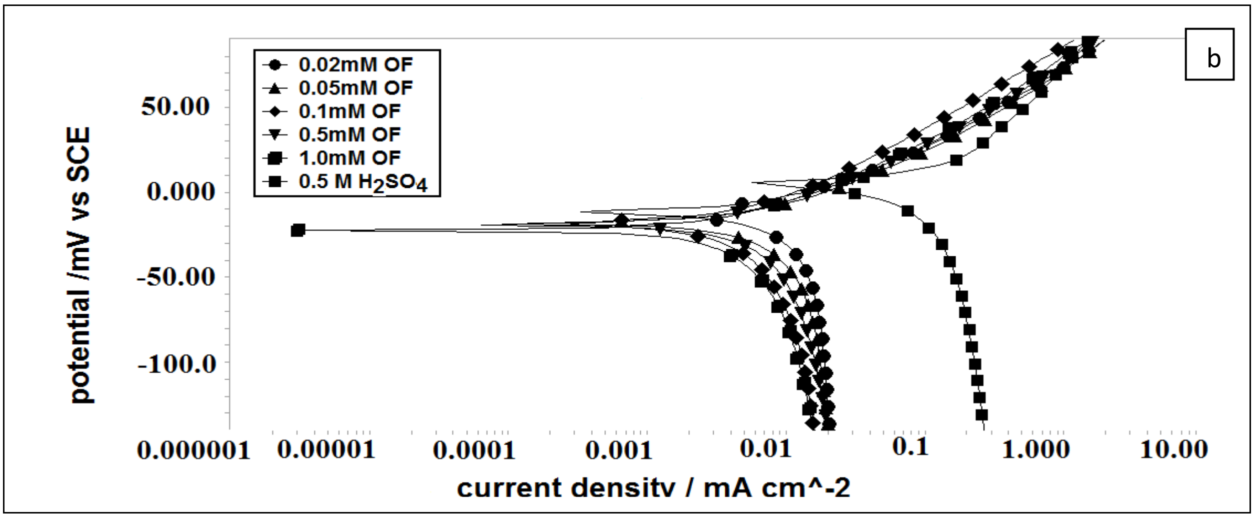

Fig. 4: Tafel plots for Cu in: (a) 1.0 M HNO_3 (b) 0.5 M H_2SO_4 solutions, at various concentrations of ofloxacin.

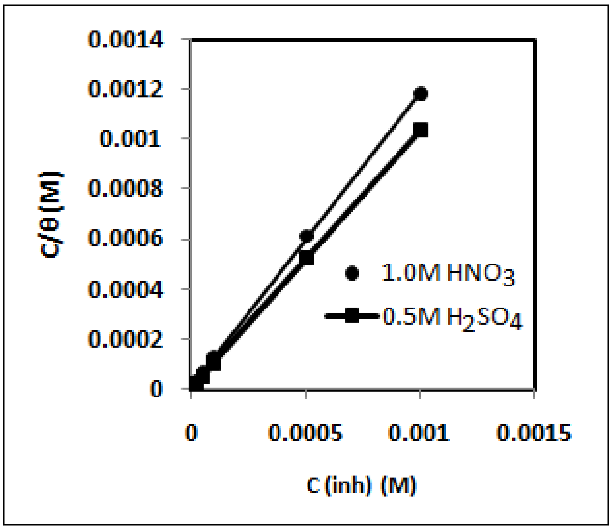

Fig. 5: Langmuir Adsorption Isotherms for the adsorption of ofloxacin onto the copper surface in 1.0 M HNO_3 and 0.5M H_2SO_4 solutions.

Table 4 has revealed that when the temperature raised the inhibitor efficacy raised; but the corrosion rate raised as well.

Figures 6 and 7 exhibit Arrhenius plots and Transition state plots, respectively. The values of E_a measured in the presence of ofloxacin were lower than those measured in the uninhibited solution, as shown in Table 5. This indicated that the energy barrier for inhibitor molecule adsorption on the nanoporous copper surface has decreased. The surface area covered by the inhibitor molecule was growing with the temperature rise and the rate of metal dissolution in corrosive fluids was regulated by corrosion product diffusion through the inhibitor molecule's protective coating (Szauer and Brandt, 1981). The fact that E_a decreased when inhibitor molecules were added to both fluids indicated that the inhibitor molecules were chemisorption-adsorbed onto the metal surface (Szauer and Brandt, 1981; Ivanov, 1986; Ma *et al.* 2003). The adsorption was an exothermic process, since ΔH was negative.

Table 4. Electrochemical parameters from Tafel polarization curves for the corrosion of copper in 1.0 M HNO_3 and 0.5 M H_2SO_4 solutions at different temperatures.

Medium	Conc. (mM)	Temperature (K)	E_{corr} (Mv)	i_{corr} µA cm^{-2}	β_C x 10^{-3} V	β_a x10^{-3} V	Corrosion rate (mpy)	IE%
HNO_3	Blank	308	2.59	30.3	173.6	54.40	49.04	-
	Blank	318	10.80	199.0	411.4	65.70	322.6	-
	Blank	328	21.70	358.0	440.0	59.90	579.2	-
	1 mM	308	-23.40	10.8	182.1	48.10	17.43	64
	1 mM	318	-3.44	22.9	174.9	45.40	36.99	88
	1 mM	328	12.70	50.6	163.1	56.40	81.70	86

H_2SO_4	Blank	308	-14.00	12.2	537.3	49.10	19.82	-
	Blank	318	-46.67	30.4	281.0	50.23	49.19	-
	Blank	328	11.70	88.5	271.9	62.89	143.2	-
	1 mM	308	-38.53	5.696	189.9	52.36	9.217	53
	1 mM	318	-38.58	6.777	223.2	48.71	10.97	78
	1 mM	328	-1.356	24.01	586.4	59.35	38.75	73

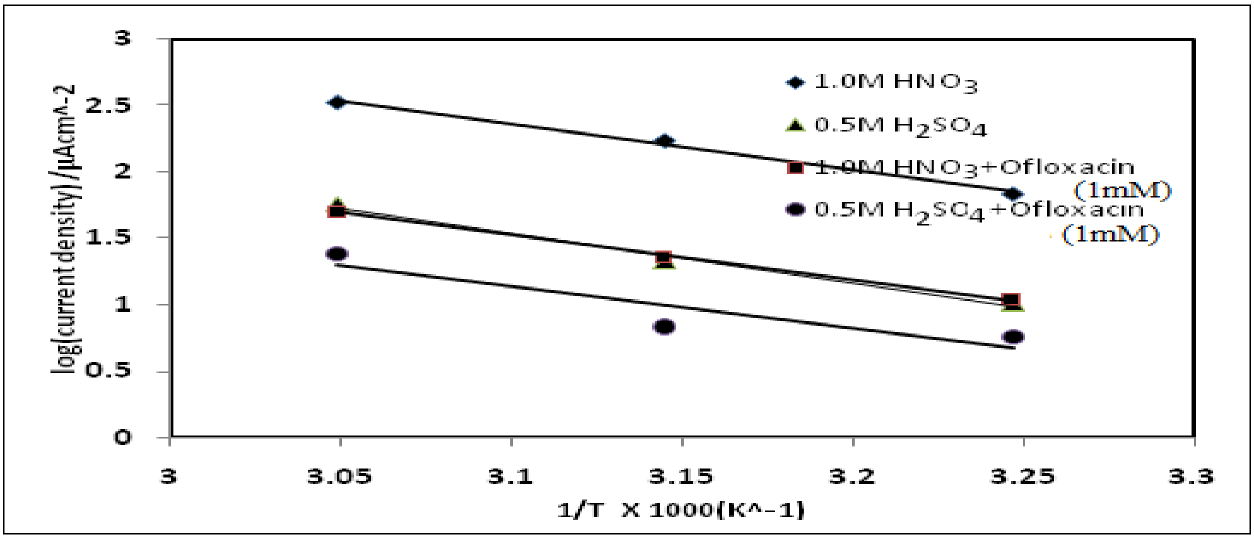

Fig. 6: Typical Arrhenius plots for corrosion of Cu in 1.0 M HNO_3 and in 0.5 M H_2SO_4 solutions.

Table 5. Thermodynamic parameters obtained from potentio-dynamic polarization studies.

Medium	Inhibitor concentration	K_{ads} (M^{-1})	ΔG_{ads} KJ/mole	ΔH KJ/mole	ΔS J/mole/K	E_a (KJ / mole)	R
HNO_3	Blank	-	-	-63.7	-26.8	66.44	0.993
	0.5 mM OF	117785	-39.14	-62.2	-28.3	64.81	0.998
H_2SO_4	Blank	-	-	-69.5	-38.2	72.19	0.989
	0.5 mM OF	518000	-42.84	-57.4	-45.4	59.94	0.826

Organic compound adsorption on metal surfaces was mostly determined by the metal's surface charge as well as the charge or dipole moment of the inhibitor molecule and other ions that are particularly adsorbed onto the metal surface (Quraishi *et al.* 2000). The open circuit potential and PZC readings were used to determine the metal's surface charge (Saliyan and Adhikari, 2008). Fig. 8 (a-d) demonstrate the dependence of the double-layer capacitance on the DC potential (d). The E_{ocp} and PZC statistics are shown in Table 6. The surface charge on copper at the open circuit potential was determined using the equation below.

$$E_r = E_{ocp} - E_{pzc} \tag{14}$$

where, E_r is Antropov's rational corrosion potential (Popova *et al.* 2003). In inhibited and uninhibited sulphuric acid and nitric acid solutions, the surface charge of copper at the OCP was found to be positive. As a result, the sulphate and nitrate ions will be adsorbed on the metal surface first (Ma *et al.* 2003; Solmaz *et al.* 2008; Saliyan and Adhikari, 2008; Popova *et al.* 2003) and the protonated inhibitor molecules make bond with the anions and retard the metal dissolution (Doner *et al.* 2011).

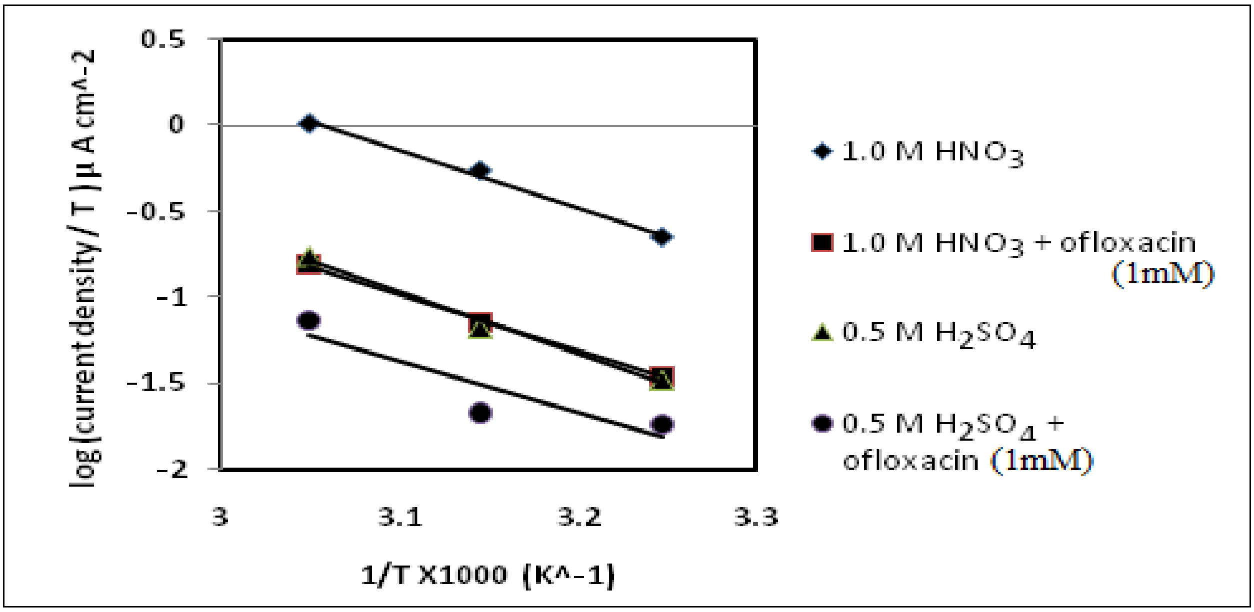

Fig. 7: The transition state plots for corrosion of Cu in 1.0 M HNO_3 and 0.5 M H_2SO_4 solutions.

Table. 6: Excess charge on Cu electrode in 1.0 M HNO_3 and 0.5 M H_2SO_4 solutions.

Medium	E_{OCP} (mv/SCE)	E_{PZC} (mv/SCE)	Excess charge (E_{OCP} - E_{PZC})
1.0 M HNO_3	42.10	+40	+2.1
1.0 M HNO_3 + 0.5 mM of inhibitor	-3.03	-220	+217
0.5 M H_2SO_4	+4.52	-20	+24.52
0.5 M H_2SO_4 + 0.5 mM of inhibitor	-18.95	-20	+1.05

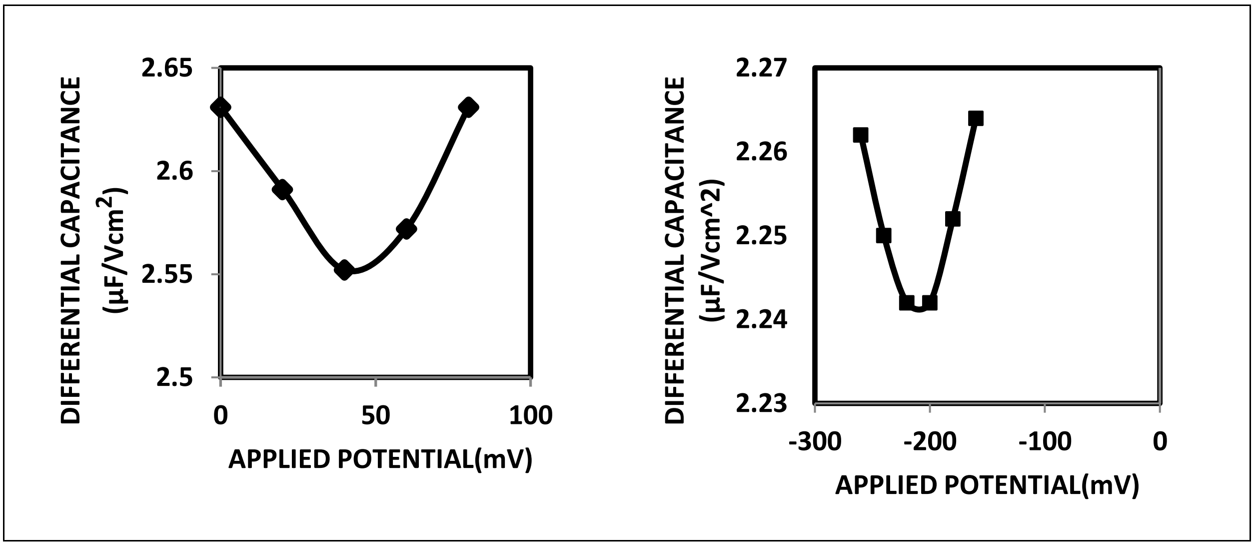

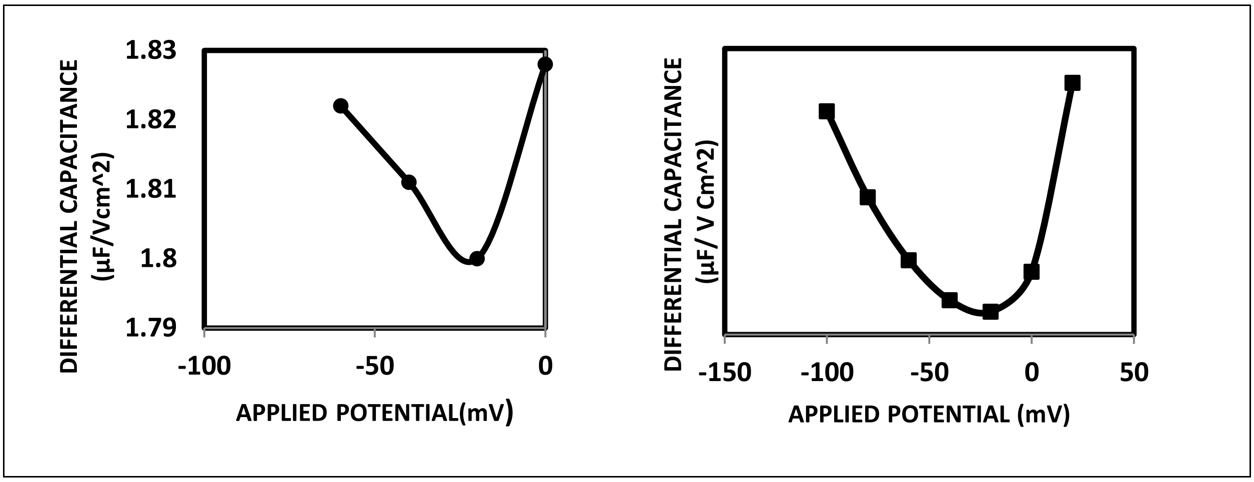

Fig. 8: The plot of differential capacitance vs. applied electrode potential for copper in: (a) 1.0 M HNO_3 solution (b) 1.0 M HNO_3 containing 0.5 mM ofloxacin (c) 0.5 M H_2SO_4 and (d) 0.5 M H_2SO_4 containing 0.5 mM ofloxacin.

3.5 Synergistic Effect of Halide Ions

When two or more corrosion inhibitors were present in a corrosive environment, synergy rather than a simple additive impact may increase inhibitor efficiency.

Since the surface charge of copper was positive, it was proposed that the halide ions will first get adsorbed onto the metal surface (Solmaz *et al.* 2008; Saliyan and Adhikari, 2008; Popova *et al.* 2003) and the protonated inhibitor molecules get adsorbed on the anions and retard the metal dissolution (Doner *et al*. 2011), as given in the equations 15 and 16:

$$X^-_S \rightarrow X^-_{ads} \quad (15)$$

$$X^-_{ads} + HI^+_S \rightarrow (X^- \text{-}HI^+)_{ads} \quad (16)$$

By establishing intermediary bridges between the metal surface and the organic inhibitor, the halide ions promote inhibitor adsorption (Ozcan *et al.* 2008; Zhao and Chen, 2012; Feng *et al.* 1999; Obot *et al.* 2009; Umoren *et al.* 2010; 2008; Pavithra *et al.* 2010; Ai *et al.* 2006). Increased surface coverage resulting from ion-pair interactions between the organic cations and the halide anions has caused corrosion inhibition synergism. Table 7 shows the synergism parameters S_θ determined from impedance investigations on the addition of KCl, KBr, and KI. According to the table, the iodide ion has a synergistic impact, but the chloride and bromide ions have an antagonistic impact in both acid media. It was due to the large ionic radius, low electronegativity and high hydrophobicity of the iodide ions (Bentiss *et al.* 2002), when compared to other halide ions, which enhances the adsorption of the inhibitor molecules onto the metal surface (Saliyan and Adhikari, 2008).

Table 7. Electrochemical parameters derived from EIS studies for the corrosion of copper in 1 M HNO_3 and 0.5 M H_2SO_4 solutions in the presence of KCl, KBr and KI.

Medium	Inhibitor Concentration (mM)	Y_0 (x 10^{-6}) $\Omega^{-1}cm^{-2}$	n	R_{ct} Ωcm^2	θ	S_θ
1.0 M HNO_3	Blank	862.9	0.997	87	-	-
	0.1 mM OF	265.2	0.961	351	0.7521	-
	0.5 mM KCl	189.1	0.898	313	0.7220	-
	0.1 mM OF + 0.5 mM KCl	120.2	0.926	198	0.5606	0.1568
	0.5 mM KBr	271.0	0.912	231.8	0.6246	-
	0.1 mM OF + 0.5 mM KBr	149.4	0.939	622.9	0.8603	0.6657
	0.5 mM KI	99.5	0.905	123	0.2926	-
	0.1 mM OF + 0.5 mM KI	55.30	0.906	1158	0.9248	2.33

0.5 M H_2SO_4	Blank	330	0.930	63	-	-
	0.1 mM OF	79.4	0.927	362	0.8259	-
	0.5 mM KCl	349.1	0.945	191	0.6701	-
	0.1 mM OF + 0.5 mM KCl	80.9	0.926	215.9	0.7081	0.1966
	0.5 mM KBr	256.7	0.934	154	0.5909	-
	0.1 mM OF + 0.5 mM KBr	84.5	0.937	584.6	0.8922	0.6604
	0.5 mM KI	152.6	0.926	174	0.6379	-
	0.1 mM OF +0.5 mM KI	45.1	0.962	2390	0.9736	2.38

3.6 Surface Morphology

SEM images of copper specimens subjected to acid solutions are shown in Fig. 9 a and Fig. 9 b. These images have demonstrated the presence of pits caused by copper corrosion in acid media. The SEM images after adding 0.5 mM ofloxacin to the corrosive medium are shown in Fig. 9 c and Fig. 9 d. Because of the protection afforded by the adsorption of inhibitor molecules onto the metal surface, no pits have emerged in these images.

3.7 Quantum Chemical Studies

Table 8 shows the theoretical parameters that were derived and offer information on the inhibitor's reactive behaviour. The energy of the highest occupied molecular orbital (E_{HOMO}) assesses a molecule's proclivity for electron donation. As a result, the higher the E_{HOMO} values, greater the inclination toward electron donation, strengthening the inhibitor's adsorption on the metal surface and therefore improving inhibitory effectiveness (Bouklah *et al.* 2012). E_{LUMO}, on the other hand, denotes the molecule's capacity to receive electrons. With raising HOMO and lowering LUMO energy levels, the inhibitor's ability to attach to the metal surface improves. Ofloxacin's lower ionization energy of 8.8950 eV has explained its increased efficiency. Ofloxacin has a softness value of 0.25100 eV and a low hardness value of 3.98400 eV, implying that it has inhibited bacteria effectively.

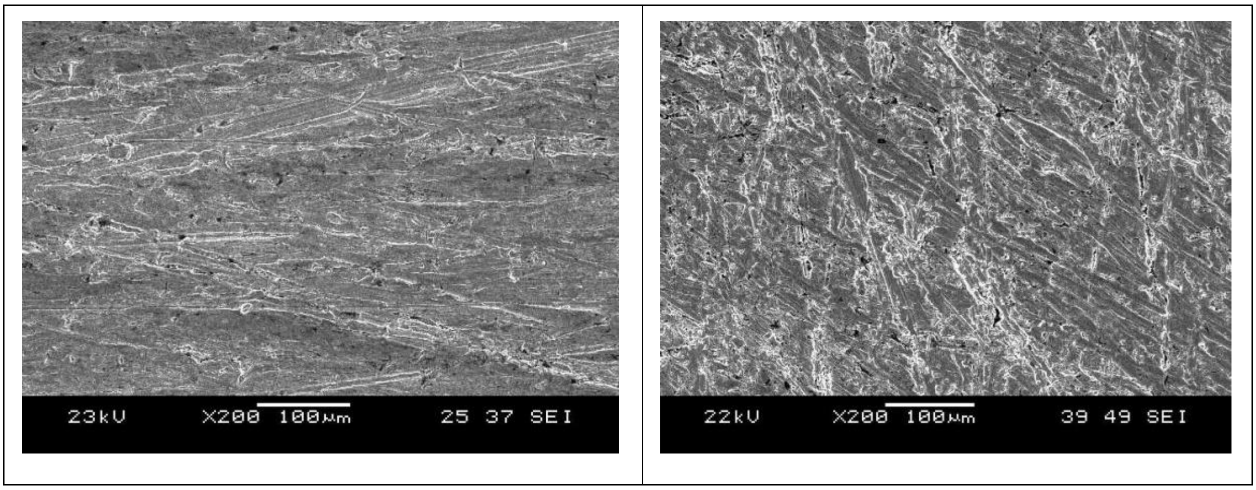

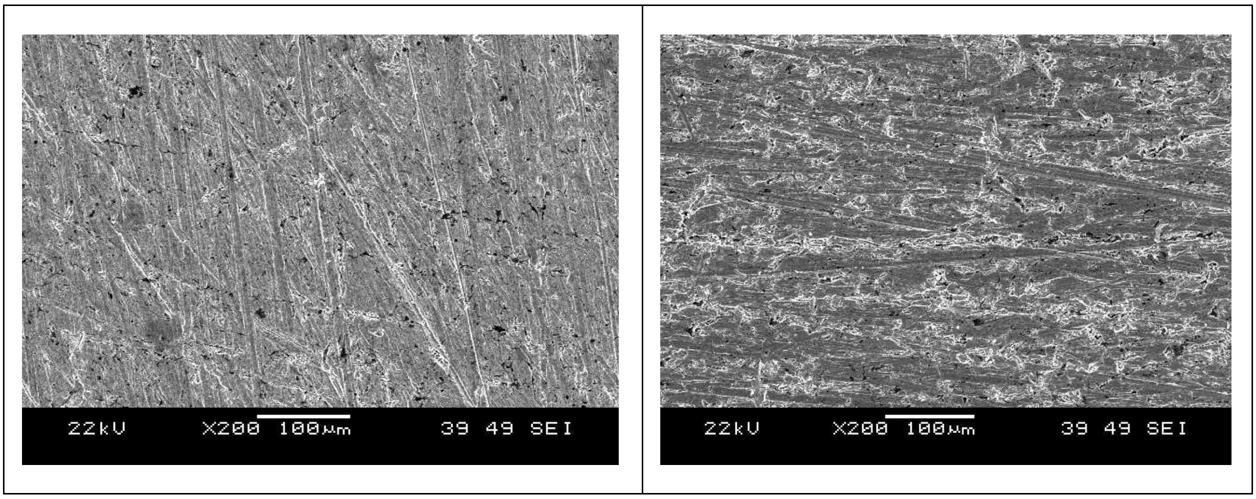

Fig. 9: SEM of copper specimen: (a) after immersion in 1.0 M HNO_3, (b) after immersion in 0.5 M H_2SO_4, (c) after immersion in 1.0 M HNO_3 containing ofloxacin and (d) after immersion in 0.5 M H_2SO_4 containing ofloxacin.

Table 8. Quantum chemical parameters of Ofloxacin

Total energy (E) (eV)	-3923.61018
Electronic energy (eV)	-30377.32
HOMO (eV)	-8.895
LUMO (eV)	-0.823
Energy gap (eV)	8.072
Ionization potential I (eV)	8.895018
Electron affinity (eV)	0.823
Electronegativity χ (eV)	4.807009
Dipole moment μ	-4.807009
Hardness η (eV)	3.984009
Softness σ (eV)	0.251003449
Electrophilicity ω (eV)	2.90000
ΔN	-0.0415

4. CONCLUSION

(i) The results have shown that the inhibitor efficiency increased with an increase in ofloxacin concentration, and ofloxacin can act as a good inhibitor for the corrosion of copper in both acid media.

(ii) EIS studies have revealed that these molecules get adsorbed onto the metal surface by replacing water molecules and act as a diffusion barrier.

(iii) The potentio-dynamic polarization studies have revealed that ofloxacin acted as a mixed type of inhibitor.

(iv) Ofloxacin adsorption has followed the Langmuir adsorption isotherm. The adsorption was spontaneous, if ΔG_{ads} values were negative.

(v) The adsorption was through chemisorption, since the value of free energy of adsorption was very close to -40 $kJmol^{-1}$.

ACKNOWLEDGEMENT

The authors gratefully acknowledge the facilities provided by the Principal and the Management of Coimbatore Institute of Technology, Tamilnadu, India and PSG College of Technology, Coimbatore, Tamilnadu, India.

FUNDING

This research received no specific grant from any funding agency in the public, commercial, or not-for-profit sectors.

CONFLICTS OF INTEREST

The authors declare that there is no conflict of interest.

COPYRIGHT

REFERENCES

Ai, J., Guo, X., Qu, J., Chen, Z. and Zheng, J., Adsorption behavior and synergistic mechanism of a cationic inhibitor and KI on the galvanic electrode, *Colloid. Surf. A: Physico.Chem. Eng. Aspect.*, 281 (1): 147-155(2006). https://doi.org/10.1016/j.colsurfa.2006.02.031

Aramaki, K. and Hackerman, N., Inhibition mechanism of medium-sized polyethyleneimine, *J. Electrochem. Soc.*, 116 (5), 568-574(1969). https://doi.org/10.1149/1.2411965

Barcia, O. and Mattos, O., Reaction model simulating the role of sulphate and chloride in anodic dissolution of iron, *Electrochim. Acta.*, 35(10), 1601-1608(1990). https://doi.org/10.1016/0013-4686(90)80016-H

Barcia, O., Mattos, O., Pebere, N. and Tribollet, B., Mass-Transport Study for the Electrodissolution of Copper in 1M Hydrochloric Acid Solution by Impedance, *J. Electrochem. Soc.*, 140(10), 2825-2832(1993). https://doi.org/10.1149/1.2220917

Benabdellah, M., Touzani, R., Aouniti, A., Dafali, A., El Kadiri, S., Hammouti, B. and Benkaddour, M., Inhibitive action of some bipyrazolic compounds on the corrosion of steel in 1M HCl: Part I: Electrochemical study, *Mater. Chem. Phys.*, 105(2): 373-379(2007). https://doi.org/10.1016/j.matchemphys.2007.05.001

Bentiss, F., Bouanis, M., Mernari, B., Traisnel, M. and Lagrenee, M., Effect of iodide ions on corrosion inhibition of mild steel by 3, 5-bis (4-methylthiophenyl)-4H-1, 2, 4-triazole in sulfuric acid solution, *J. Appl. Electrochem.*, 32(6), 671-678 (2002). https://doi.org/10.1023/A:1020161332235

Bentiss, F., Traisnel, M., Gengembre, L. and Lagrenée, M., A new triazole derivative as inhibitor of the acid corrosion of mild steel: electrochemical studies, weight loss determination, SEM and XPS, *Appl. Surf. Sci.*, 152(3), 237-249(1999). https://doi.org/10.1016/S0169-4332(99)00322-0

Bouklah, M., Harek, H., Touzani, R., Hammouti, B. and Harek, Y., DFT and quantum chemical investigation of molecular properties of substituted pyrrolidinones, *Arab. J. Chem.*, 5(2), 163-166 (2012). https://doi.org/10.1016/j.arabjc.2010.08.008

Döner, A., Solmaz, R., Özcan, M. and Kardaş, G., Experimental and theoretical studies of thiazoles as corrosion inhibitors for mild steel in sulphuric acid solution, *Corros. Sci.*, 53(9), 2902-2913(2011). https://doi.org/10.1016/j.corsci.2011.05.027

Feng, Y., Siow, K., Teo, W. and Hsieh, A., The synergistic effects of propargyl alcohol and potassium iodide on the inhibition of mild steel in 0.5 M sulfuric acid solution, *Corros. Sci.*, 41(5), 829-852(1999). https://doi.org/10.1016/S0010-938X(98)00144-9

Ferreira, E., Giacomelli, C., Giacomelli, F. and Spinelli, A., Evaluation of the inhibitor effect of L-ascorbic acid on the corrosion of mild steel, *Mater. Chem. Phys.*, 83(1), 129-134(2004). https://doi.org/10.1016/j.matchemphys.2003.09.020

Gao, J., Methods and applications of combined quantum mechanical and molecular mechanical potentials, *Rev. Comput. Chem.*, **7,** 119-186(1996). https://doi.org/10.1002/9780470125847.ch3

Geerlings, P., De Proft, F. and Langenaeker, W., Conceptual density functional theory, *Chem. Rev.*, 103(5), 1793-1874(2003). https://doi.org/10.1021/cr990029p

Hosseini, M., Mertens, S. F., Ghorbani, M. and Arshadi, M. R., Asymmetrical Schiff bases as inhibitors of mild steel corrosion in sulphuric acid media, *Mater. Chem. Phys.*, 78(3), 800-808(2003). https://doi.org/10.1016/S0254-0584(02)00390-5

Hsu, C. and Mansfeld, F., Technical note: concerning the conversion of the constant phase element parameter Y_0 into a capacitance, *Corrosion.*, 57(9), 747-748(2001). https://doi.org/10.5006/1.3280607

Ivanov, E., Inhibitors for metal corrosion in acid media, *Metallurgy*, Moscow, (1986).

Joseph, B. and Joseph, A., Inhibition of Copper Corrosion in 1 M Nitric Acid-Electro Analytical and Theoretical Study with (E)-(4-(4-Methoxybenzylideneamino)-4H-1, 2, 4-Triazole-3, 5diyl) Dimethanol (MBATD), *Port. Electrochim. Acta.*, 29(4), 253-271(2011). https://doi.org/10.4152/pea.201104253

Khaled, K., Corrosion control of copper in nitric acid solutions using some amino acids–A combined experimental and theoretical study, *Corros. Sci.*, 52(10), 3225-3234(2010). https://doi.org/10.1016/j.corsci.2010.05.039

Li, W-h., He, Q., Zhang, S-t., Pei, C-l. and Hou, B-r., Some new triazole derivatives as inhibitors for mild steel corrosion in acidic medium, *J. Appl. Electrochem.*, 38(3), 289-295(2008). https://doi.org/10.1007/s10800-007-9437-7

Li, X., Deng, S. and Fu, H., Synergism between red tetrazolium and uracil on the corrosion of cold-rolled steel in H_2SO_4 solution, *Corros. Sci.*, 51(6), 1344-1355(2009). https://doi.org/10.1016/j.corsci.2009.03.023

Ma, H., Chen, S., Niu, L., Zhao, S., Li, S. and Li, D., Inhibition of copper corrosion by several Schiff bases in aerated halide solutions, *J. Appl. Electrochem.*, 32(1), 65-72(2002). https://doi.org/10.1023/A:1014242112512

Ma, H., Chen, S., Yin, B., Zhao, S. and Liu, X., Impedance spectroscopic study of corrosion inhibition of copper by surfactants in the acidic solutions, *Corros. Sci.*, 5(5), 867-882(2003). https://doi.org/10.1016/S0010-938X(02)00175-0

Obot, I., Obi-Egbedi, N. and Umoren, S., The synergistic inhibitive effect and some quantum chemical parameters of 2,3-diaminonaphthalene and iodide ions on the hydrochloric acid corrosion of aluminium, *Corros. Sci*., 51(2), 276-282(2009). https://doi.org/10.1016/j.corsci.2008.11.013

Özcan, M., Solmaz, R., Kardaş, G. and Dehri, I., Adsorption properties of barbiturates as green corrosion inhibitors on mild steel in phosphoric acid, *Colloid. Surf. A: Physico. Chem. Eng. Aspect*., 325(1), 57-63(2008). https://doi.org/10.1016/j.colsurfa.2008.04.031

Pavithra, M., Venkatesha, T., Vathsala, K. and Nayana, K., Synergistic effect of halide ions on improving corrosion inhibition behaviour of benzisothiozole-3-piperizine hydrochloride on mild steel in 0.5 MH_2SO_4 medium, *Corros. Sci*., 52 (11), 3811-3819(2010). https://doi.org/10.1016/j.corsci.2010.07.034

Popova, A., Sokolova, E., Raicheva, S. and Christov, M., AC and DC study of the temperature effect on mild steel corrosion in acid media in the presence of benzimidazole derivatives, *Corros. Sci*., 45(1), 33-58(2003). https://doi.org/10.1016/S0010-938X(02)00072-0

Quraishi, M., Rawat, J. and Ajmal, M., Dithiobiurets: a novel class of acid corrosion inhibitors for mild steel, *J. Appl. Electrochem*., 30(6), 745-751(2000). https://doi.org/10.1023/A:1004099412974

Rahman, K., Schneider, S. C. and Seitz, M. A., Hopping and Ionic Conduction in Tin Oxide-Based Thick-Film Resistor Compositions, *J. Am. Ceram. Soc.*, 80(5), 1198-1202(1997). https://doi.org/10.1111/j.1151-2916.1997.tb02964.x

Şahin, M., Bilgic, S. and Yılmaz, H., The inhibition effects of some cyclic nitrogen compounds on the corrosion of the steel in NaCl mediums, *Appl. Surf. Sci.*, 195(1), 01-07(2002). https://doi.org/10.1016/S0169-4332(01)00783-8

Saiyan, V. R. and Adhikari, A. V., Quinolin-5-ylmethylene-3-{[8-(trifluoromethyl) quinolin-4-yl] thio} propanohydrazide as an effective inhibitor of mild steel corrosion in HCl solution, *Corros. Sci.*, 50(1), 55-61(2008). https://doi.org/10.1016/j.corsci.2006.06.035

Sanghvi, M., Shukla, S., Misra, A., Padh, M. and Mehta, G., Inhibition of hydrochloric acid corrosion of mild steel by aid extracts ofembilica officianalis, Terminalia bellirica and Terminalia chebula, *Bull. Electrochem*., 13(8-9), 358-361(1997).

Solmaz, R., Kardaş, G., Culha, M., Yazıcı, B. and Erbil, M., Investigation of adsorption and inhibitive effect of 2-mercaptothiazoline on corrosion of mild steel in hydrochloric acid media, *Electrochim. Acta*., 53(20), 5941-5952(2008). https://doi.org/10.1016/j.electacta.2008.03.055

Sauer, T. and Brandt, A., Adsorption of oleates of various amines on iron in acidic solution, *Electrochim. Acta*., 26(9), 1253-1256(1981). https://doi.org/10.1016/0013-4686(81)85107-9

Umoren, S, Li, Y & Wang, F. 'Synergistic effect of iodide ion and polyacrylic acid on corrosion inhibition of iron in H_2SO_4 investigated by electrochemical techniques. *Corros. Sci*.; 52(7): 2422-2429(2010). https://doi.org/10.1016/j.corsci.2010.03.021

Umoren, S., Ogbobe, O., Igwe, I. and Ebenso, E., Inhibition of mild steel corrosion in acidic medium using synthetic and naturally occurring polymers and synergistic halide additives, *Corros. Sci*.; 50 (7): 1998-2006(2008). https://doi.org/10.1016/j.corsci.2008.04.015

Yurt, A., Bereket, G., Kivrak, A., Balaban, A. and Erk, B., Effect of Schiff bases containing pyridyl group as corrosion inhibitors for low carbon steel in 0.1 M HCl, *J. Appl. Electrochem*., 35(10), 1025-1032 (2005). https://doi.org/10.1007/s10800-005-7336-3

Zarrouk, Hammouti, B., Zarrok, H., Bouachrine, M., Khaled, K. and Al-Deyab, S., Corrosion inhibition of copper in nitric acid solutions using a new triazole derivative, *Int. J. Electrochem. Sci*., 7(1), 89-105(2012).

Zhao, J. and Chen, G., The synergistic inhibition effect of oleic-based imidazoline and sodium benzoate on mild steel corrosion in a CO_2-saturated brine solution, *Electrochim. Acta*., 69, 247-255(2012). https://doi.org/10.1016/j.electacta.2012.02.101